# Inter-Robots Position Estimation Using UWB Positioning Devices for Distributed Cooperative Control of Multiple Robots

Airi Kojima, Kohei Yamagishi, Tsuyoshi Suzuki
Department of Information and Communication Engineering,
Tokyo Denki University, Tokyo, Japan

***Abstract*—Ultra-wide band (UWB)-based positioning methods for static environments have been continuously improved; however, many existing approaches rely on fixed reference nodes, and methods for directly computing relative positions among mobile units have not been sufficiently investigated. This paper presents a relative positioning approach for multi-robot systems using UWB wireless communication within a distributed cooperative control framework. In the proposed approach, multiple UWB positioning devices are arranged in regular polyhedral configurations to improve the uniformity of ranging accuracy. Robot coordinates are estimated using a nonlinear least-squares optimization method formulated from a system of simultaneous distance equations, enabling mutual relative position estimation among robots. Simulation experiments were conducted to evaluate estimation accuracy and error characteristics under different geometric configurations. Four configurations: square, tetrahedron, regular tetrahedron, and regular octahedron were considered, and their error magnitudes and axis-wise distributions were compared. The simulation results indicate that the proposed configuration achieve lower estimation errors than the other configurations evaluated. Based on these findings, experimental verification was performed, and the observed trends were consistent with the simulation results. This work provides a systematic investigation of a mutual positioning system that enables robots to estimate their positions with respect to one another without relying on fixed landmarks. Unlike existing method, our approach enables the determination of relative positions between robots based on distances measured by each robot. The proposed approach is expected to be applicable to autonomous decentralized control in multi-robot systems operating in static environments.**

***Keywords*—Mobile robots; distributed cooperative control; mutual positioning system; relative position estimation; UWB positioning devices; geometric structure**

## I. Introduction

Autonomous decentralized systems that operate multiple robots are being applied to distributed tasks, such as logistics systems, which cannot be effectively addressed by individual robot [1]. In such systems, robots recognize one another in an environment populated by multiple agents and adapt their actions based on exchanged information, resulting in the achievement of shared objectives [2]. In natural ecosystems, such interactions generate collective behavior that sustains life within a herd. When applied to robotic systems, this approach allows coordinated behavior to be adjusted in a self-organized manner when part of the system fails or the environment changes, thereby enhancing flexibility, diversity, and fault tolerance [3]. In an ideal autonomous decentralized system, each robot cooperates autonomously with surrounding robots to achieve the objectives of the overall system [4].

This interaction relies on localized sensing and communication, enabling robots to recognize and exchange information with each other. While this requirement can be addressed through global observation and network-based broadcasting using camera- and network-based systems, such approaches face challenges due to the complexity of robot and systems [5]. To overcome these challenges, an ideal distributed cooperative system based on local robotic interactions is required.

To implement such distributed cooperative control, each robot should be equipped with two types of devices: one for recognizing surrounding robots and the environment, and another for local communication with neighboring robots [6]. Existing implementations often rely on multiple devices for recognizing objects using LiDAR [7] and GNSS [8], and for communication using Bluetooth and other communication technologies [9]. However, this results in increased system complexity and limited stability [10]. Therefore, a unified solution that enables both sensing and communication is desirable.

Ultra-wideband (UWB) wireless communication devices have attracted attention as promising candidates for such unified solutions. In addition to providing wireless communication, UWB technology enables highly accurate positioning by measuring time differences in the arrival of radio waves [11], [12]. This capability allows a single UWB device to support both communication and positioning for decentralized control of multiple robots, eliminating the need for multiple devices [13].

This paper proposes a method for estimating the three-dimensional relative positions of multiple robots using UWB positioning devices. Our primary contribution is the development of a technique that enables each robot to estimate relative position to other robots, thereby facilitating effective autonomous decentralized control in systems comprising two or more robots. Unlike existing approaches, the proposed method enables the determination of positions between neighboring robots based on the distance information collected by each robot.

The remainder of this paper is organized as follows. Section II reviews related work. Section III presents a method for estimating the three-dimensional relative positions between multiple robots. Section III-A describes the system design, and Section III-B provides a detailed explanation of the methodology. Sections IV and V present simulations using the error characteristics of UWB technology and experiments conducted using actual hardware, along with the results. Finally, the conclusions and future work are discussed in Sections VI and VII, respectively.

## II. Related Work

Various approaches have been proposed to realize sensing and communication for distributed multi-robot systems. For positioning, a range of devices has been explored, including LiDAR and GNSS, while Bluetooth and other wireless technologies have been investigated for inter-robot communication. However, a robot configuration that relies on multiple heterogeneous devices increases system complexity and reduces overall stability.

Conventional UWB-based positioning methods typically involve placing fixed devices at the same height at the four corners of a positioning space, as illustrated in Fig. 1a, while mobile devices move within this space [14]. The coordinate of each mobile device is calculated based on the absolute coordinates of the fixed devices measured by the UWB devices. However, when all fixed devices are positioned at the same height, accurate estimation of vertical position becomes difficult.

To address this limitation, Zhou *et al*. demonstrated that positioning accuracy can be improved by varying the heights of the fixed devices, as illustrated in Fig. 1b [15]. Furthermore, positioning methods using UWB devices in static environments are being continually improved, and some studies have extended these approach to relative positioning by incorporating triangulation techniques [16]. In such methods, four devices measure the distances between one another to estimate their relative positions, enabling applications to systems comprising four or more robots.

In addition, relative position estimation methods for robots equipped with multiple UWB devices has been developed [17]. This involved a system in which one robot is equipped with a fixed reference device, as shown in Fig. 1c, which enables it to estimate the position of other robots. However, because one unit functions as a landmark, mutual localization among robots has not yet been investigated.

In contrast to these existing approaches, this study focuses on mutual relative position estimation among multiple robots using UWB devices, without relying on fixed landmarks or global references.

## III. Proposed Method

### A. System Configuration

Each node is equipped with a positioning system in which the transmitting UWB device are positioned at the vertices of a regular polyhedron, as illustrated in Fig. 2, while a receiving UWB device is positioned at the center of the regular polyhedron. This configuration ensures that the transmitters are uniformly distributed over the entire perimeter, thereby improving ranging accuracy [18]. Within the environment where a node is located, the node can measure the relative distance of transmitters belonging to other nodes using its self-mounted receiver. If the coordinate system of the regular polyhedron formed by the transmitters is known, the relative coordinates to another node can be obtained by calculating the intersection of the distances between the receiver and transmitters.

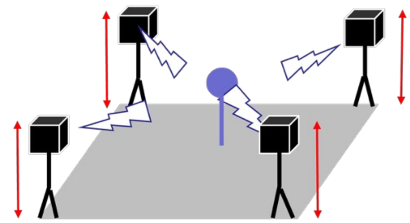

(a) Conventional positioning systems.

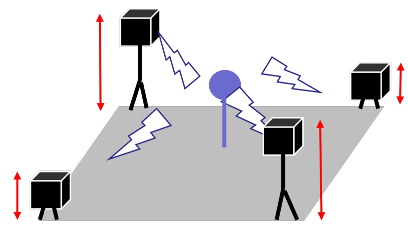

(b) Improved conventional positioning system.

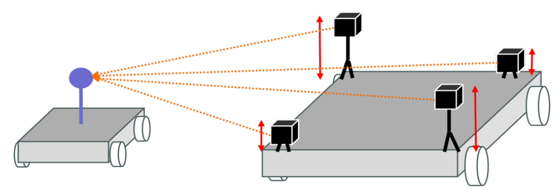

(c) Positioning that enables robots to know each other's locations.

Fig. 1. UWB positioning device placement method.

Conventional UWB-based positioning methods require four or more reference points to identify spatial coordinates [19]. Similarly, GNSS-based systems employ four-point surveying, in which distances to four satellites are measured to determine position [20]. This principle is also applied to UWB systems because it enables more efficient and accurate spatial coordinate estimation than conventional techniques.

### B. Coordinates Calculation-Based on n-Polyhedron

Based on this principle, the proposed method utilizes distance measurements from a minimum of $n = 4$ transmitters to estimate the the three-dimensional coordinates $(x, y, z)$ of the receiver. Let the coordinates of the transmitters be $(x_1, y_1, z_1)$, $(x_2, y_2, z_2)$, ..., $(x_n, y_n, z_n)$, and let the measured distances between the receiver and each transmitter be $r_1$, $r_2$, ..., $r_n$. This receiver position satisfies the following system of $n$ equation:

$$\left.\begin{aligned}(x-x_1)^2+(y-y_1)^2+(z-z_1)^2-r_1^2=0\\(x-x_2)^2+(y-y_2)^2+(z-z_2)^2-r_2^2=0\\\vdots\qquad\qquad\\(x-x_n)^2+(y-y_n)^2+(z-z_n)^2-r_n^2=0\end{aligned}\right\}\tag{1}$$

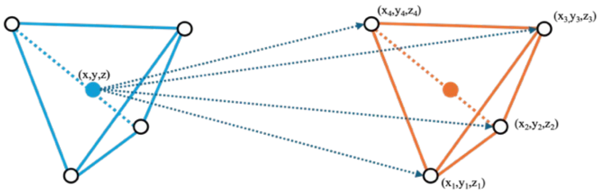


(a) Tetrahedron (with four devices).

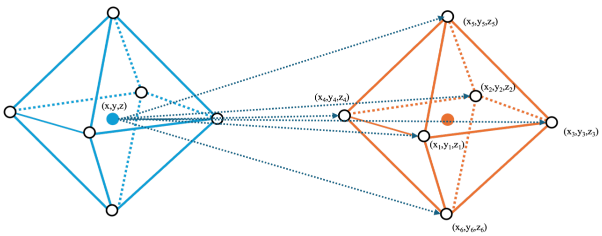


(b) Octahedron (with six devices).

Fig. 2. Component systems.

Theoretically, based on Eq. (1), only one spatial coordinate can be determined. However, in practical scenarios, measurement errors are superimposed on the observed distances, and the system of equation is not satisfied exactly. In this study, an approximate solution is obtained by solving a nonlinear least-squares problem. The measured distances $r_i$ are used as initial values, and the solution is iteratively refined until convergence to the coordinates $(x, y, z)$ that best satisfy Eq. (1).

## IV. Comparison of Errors by Simulation

### A. Experimental Overview

Simulations were conducted to evaluate the extent to which the proposed method reduces estimation error compared to the conventional methods. Specifically, the variation in error with respect to geometric shape and size was analyzed.

The following configurations were compared: a square configuration representing the conventional method, in which the transmitting devices arranged on the same plane; a tetrahedral configuration similar to the conventional method but with different device heights, and proposed configurations using a regular tetrahedron (Fig. 2a) and a regular octahedron (Fig. 2b).

As part of the experimental conditions, the length of one side of each configuration was set to 0.25 and 0.5 m. These values were selected because the proposed system is intended for estimating the relative positions of mobile robots, and thus the onboard positioning system must be as compact as possible. The distance between the receiving and transmitting devices was varied from 0 to 20 m in increments of 0.2 m. For each condition, the calculation was repeated 100,000 times, and the average error was computed.

All simulations were performed using Python 3.7.9, with the Numpy 1.21.6 and Scipy 1.7.3 libraries.

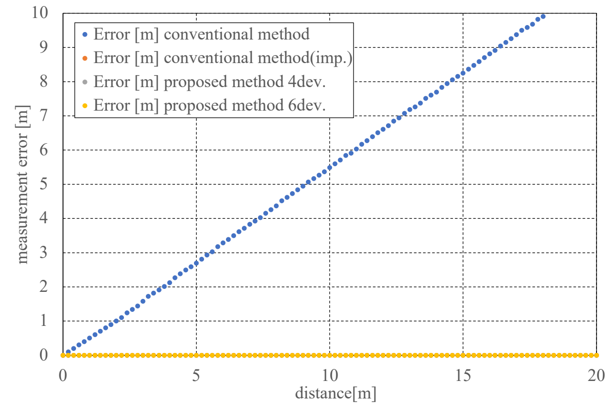


(a) Side length: 0.25 m.

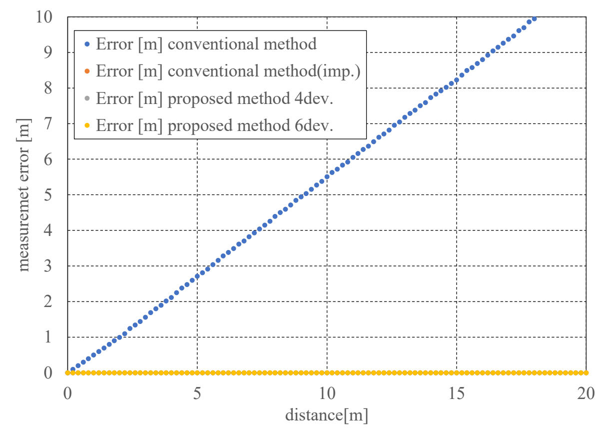


(b) Side length: 0.5 m.

Fig. 3. Experimental results (without error).

### B. Experimental Results

The simulation results showing the change in error with the distance are presented in Fig. 3. Fig. 3a and 3b correspond to side lengths of 0.25 and 0.5 m. For the conventional square configuration, the estimation error increases proportionally with distance, regardless of side length. In contrast, the errors associated with the other configurations remain almost negligible. These results indicate that three-dimensional configurations, such as the tetrahedral and octahedral arrangements, provide improved ranging accuracy compared with the planar square configuration.

Fig. 4 presents the results of simulations evaluating the effect of mixed measurement errors. In these simulations, a measurement error with a standard deviation of 0.01 m was superimposed on the ranging distance $r_i$, corresponding to a $1\sigma$ uncertainty. Given that UWB positioning typically achieves accuracy on the order of several centimeters, a minimum error of 0.01 m was added to the distance measurements to account for realistic measurement uncertainty [21].

Under these conditions, the square configuration exhibited the largest estimation error, whereas the regular polyhedral configurations proposed in this paper demonstrated smaller errors than both the square and tetrahedral configurations. Among the regular polyhedrons, the regular octahedron con-

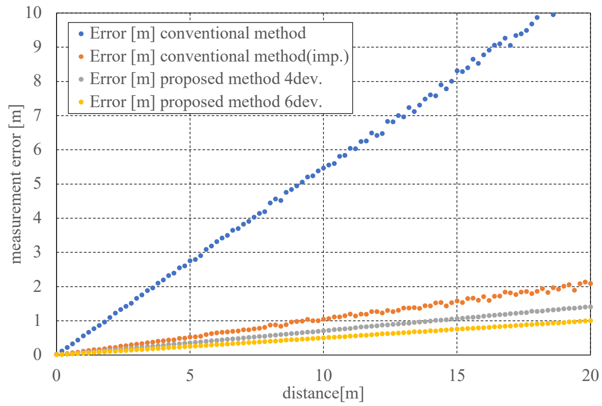


(a) Side length: 0.25 m.

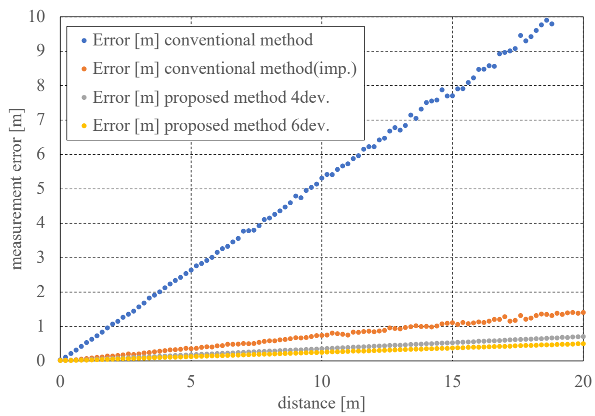


(b) Side length: 0.5 m.

Fig. 4. Experimental results (mixing error: 0.01 m).

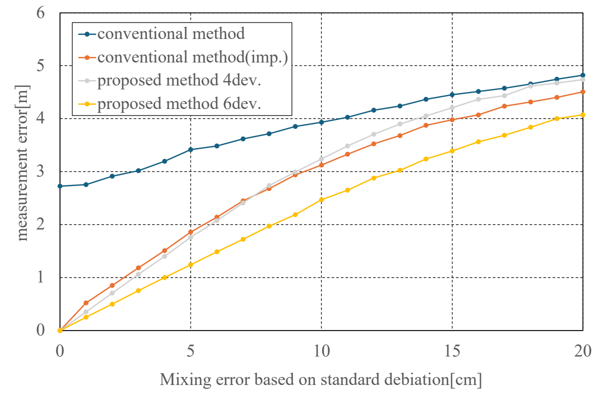


(a) Side length: 0.25 m.

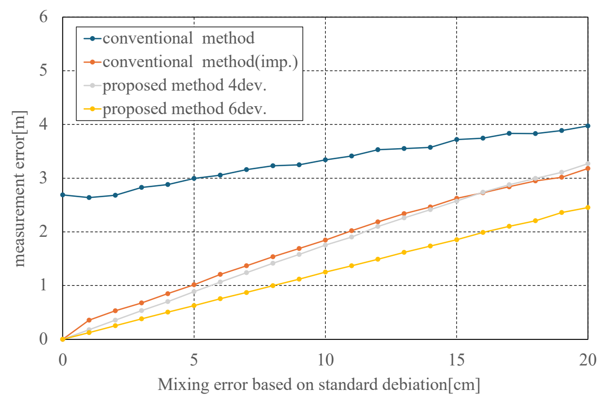


(b) Side length: 0.5 m.

Fig. 5. Comparison of errors by mixing error (5m point).

sistently yielded lower errors than the regular tetrahedron. This improvement can be attributed to the increased number of equations resulting from a larger number of positioning devices.

The effects of increasing mixed error magnitude are shown in Fig. 5. Fig. 5a and 5b correspond to side lengths of 0.25 and 0.5 m, respectively. In both cases, the square configuration produced the largest error, consistent with the trends shown in Fig. 3 and 4. As the mixed error increased, the estimation errors for the tetrahedral configuration and the proposed regular tetrahedral configuration gradually converged. For the 0.25-m condition, the error associated with the tetrahedral configuration exceeded that of the square configuration when the mixed error exceeded 0.13 m. This discrepancy is attributed to the sensitivity of the optimization process to the initial values used in the simulation. At a mixed error of 0.13 m, the resulting error range was approximately 0.4 m, rendering the system unsuitable for practical distance measurement.

For the 0.5-m condition, both the tetrahedral and octahedral configurations exhibited increased estimation error as the mixed error increased. However, unlike the 0.25-m condition, the square and tetrahedral configurations demonstrated smaller changes in error compared with the regular tetrahedral configuration. Among the regular polyhedrons, the regular octahedral configuration demonstrated lower errors and higher accuracy than the regular tetrahedral configuration, as shown in Fig. 3.

Both the theoretical and experimental results, even with accounting for measurement errors, indicate that proposed regular polyhedral configurations yield smaller estimation errors. Compared with conventional methods, the use of regular octahedrons reduced the estimation error by approximately half. These results demonstrate that the regular polyhedral configuration employed in the proposed method enhances the accuracy of relative position estimation and reduces sensitivity to measurement noise.

Fig. 6 shows the simulation results for error distribution along each coordinate axis, obtained using theoretical distances without mixed errors. Fig. 6b and 6c show the results for the proposed regular tetrahedral and octahedral configurations, respectively. Fig. 6 illustrates the squared error for each configuration under the conditions with a side length of 0.5 m. By analyzing the squared error, the contribution of each axis to the overall estimation error can be evaluated.

As shown in Fig. 6a, the square configuration exhibits minimal errors along the $x$- and $y$-axes, while most of the error is concentrated along the $z$-axis. This indicates that the conventional square configuration significantly degrade the position estimation with respect to height. In contrast, the tetrahedral

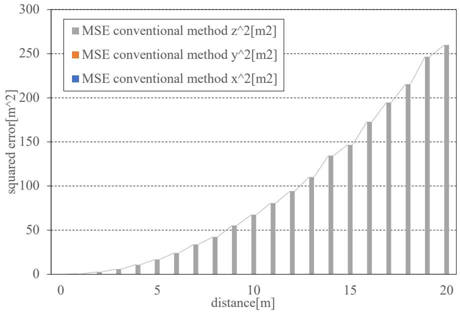


(a) Conventional method (square).

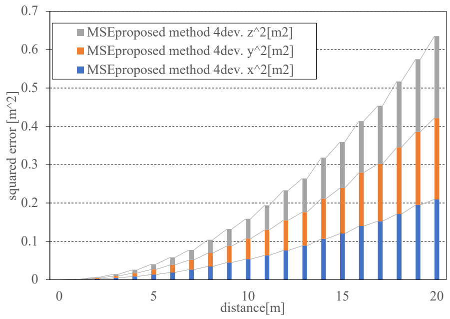


(b) Proposed method with four devices (tetrahedron).

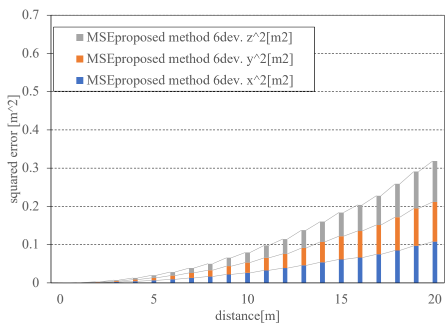


(c) Proposed method with six devices (octahedron).

Fig. 6. Comparison of errors by squared error.

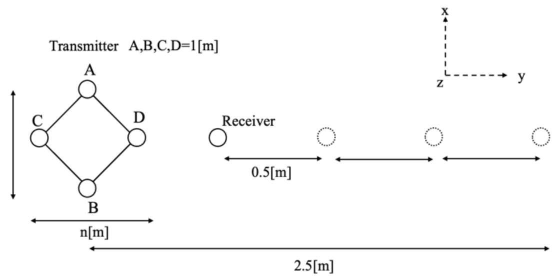


(a) Conventional method (square).

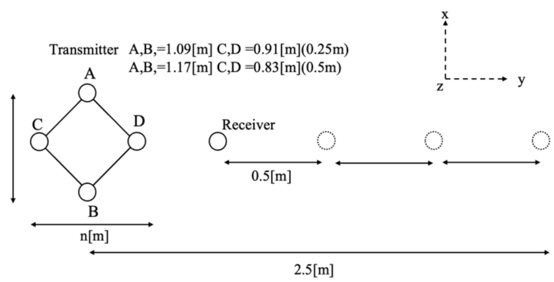


(b) Proposed method with four devices (tetrahedron).

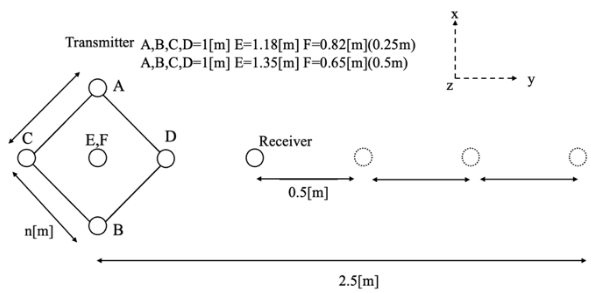


(c) Proposed method with six devices (octahedron).

Fig. 7. Illustrated summary of experiment: $n$ in the figure changes the length of a side depending on the experimental conditions.

and octahedral configurations exhibit more balanced error distributions across each axis, with overall error magnitudes smaller than those of the conventional configulation.

These results demonstrate that the proposed method more effectively reduces estimation error and achieves a more uniform error distribution across all axises than the conventional methods. Consequently, the use of regular polyhedral configurations improves position estimation performance and enables more reliable and uniform ranging.

## V. Field Experiments

### A. Experimental Overview

Field experiments using UWB positioning devices were conducted to compare the positioning errors of the conventional and proposed methods based on actual measurements. The UWB device used in this study was the type 2AB module manufactured by Murata, which incorporates the Qorvo QM33120W UWB chip [22].

For the conventional method using a square configuration, the transmitting devices were arranged with side lengths of either 0.25 or 0.5 m. Because multiple placement planes are possible for the square configuration, positioning experiments were conducted in both the $xy$-plane and $xz$-planes. For the proposed method, regular polyhedral configurations were employed under the same conditions as those used in the simulations, specifically tetrahedral and octahedral arrangements. Regular tetrahedron and octahedron with side lengths of 0.25 or 0.5 m were constructed, with UWB modules placed at each vertex as transmitting devices.

In all configurations, the receiving device was fixed at a height of 1 m, and the distance from the center of the unit was varied from 1.0 m to 2.5 m in increments of 0.5 m. The maximum distance was limited to 2.5 m because the experiments were conducted within the measurable range achievable under the regular polyhedral configuration. Each experimental deployment consisted of multiple positioning

TABLE I. MEASUREMENT ERROR IN LINEAR DISTANCE FOR EACH SHAPE (SIDE LENGTH: 0.25 M)

| Distance [m] | Measurement Error[m] | | | |
|---|---|---|---|---|
| | Conventional method | | Proposed method | |
| | xy-plane | xz-plane | 4 devices | 6 devices |
| 1 | 0.995 | 1.000 | 0.212 | 0.403 |
| 1.5 | 1.479 | 1.500 | 0.238 | 0.389 |
| 2 | 1.983 | 1.933 | 0.427 | 0.395 |
| 2.5 | 2.479 | 2.338 | 0.575 | 0.739 |

TABLE II. MEASUREMENT ERROR IN LINEAR DISTANCE FOR EACH SHAPE (SIDE LENGTH: 0.5 M)

| Distance [m] | Measurement Error[m] | | | |
|---|---|---|---|---|
| | Conventional method | | Proposed method | |
| | xy-plane | xz-plane | 4 devices | 6 devices |
| 1 | 0.995 | 1.000 | 0.108 | 0.191 |
| 1.5 | 1.492 | 1.500 | 0.198 | 0.131 |
| 2 | 1.988 | 2.000 | 0.395 | 0.247 |
| 2.5 | 2.483 | 2.500 | 0.491 | 0.436 |

points comprising a set of transmitter devices and a single receiver. A schematic of the experimental setup is shown in Fig. 7. All experiments were conducted in a lecture room at the Tokyo Senju Campus of Tokyo Denki University.

For evaluation, 500 datasets were collected for each condition, and the positioning error was calculated using the non-linear least-squares method. The mean error and the universal standard deviation were used as evaluation metrics. Python 3.7.9 was used for optimization, and the least-squares solution was computed using the Scipy 1.7.3 library.

### B. Experimental Overview

Tables I and II present the linear distance errors calculated using for each configuration. The results show that both the tetrahedral and octahedral configurations yield reduced errors compared with the square configuration. A comparison between the $xy$- and $xz$-plane arrangements indicates that the error does not differ significantly between them, although slightly lower errors were observed in the $xy$-plane. Furthermore, a comparison between the tetrahedral and octahedral configurations revealed that, in contrast to the simulation results, the tetrahedral configuration produced smaller errors than the octahedral configuration in the field experiments. This discrepancy is attributed to the measurement noise in the actual ranging data, whose influence depends on the magnitude of the measurement error. In addition, the observation that the errors were smaller for a side length of 0.5 m than for 0.25 m can be explained by the resolution of the UWB device used in this study, which measures distance with centimeter-level granularity.

Fig. 8 shows a comparison of the squared error components for each axis. Similar to the linear distance error, the squared errors were smaller for the tetrahedral and octahedral configurations than the square configuration. The squared errors for the square configurations were larger for the $xz$-plane than for the $xy$-plane. In Fig. 8a, errors occurred predominantly along the $y$-axis. This behavior can be attributed to the fact that the transmitting device farthest from the receiving device was located along the $y$-axis, making the measurements more susceptible to interference from radio waves generated by other wireless communication systems. In Fig. 8b, the squared errors were distributed across both the $x$- and $z$-axes. Unlike Fig. 8a, where the distances between the transmitting and receiving devices were uniform, the presence of similar measurement errors across all ranging data in the $xz$-plane led to the error distribution shown in Fig. 8b.

Subsequently, the results of the proposed polyhedral configurations are discussed. Notably, although the octahedral configuration exhibited relatively large linear distance errors at a distance of 1 m, its squared error was smaller than that of the tetrahedral configuration. This behavior is attributed to the proximity of transmitting device C to the receiving device in the octahedral configuration, which results in less stable measurements at short distances. However, at other measurement points, the octahedral configuration yielded smaller errors, leading to reduced least-squares error values consistent with the simulation results.

In the conventional square configuration, estimation errors tend to accumulate along specific axes, making accurate three-dimensional relative position estimation difficult. In contrast, the proposed regular polyhedral configurations reduce error components along each axis, enabling more accurate and balanced three-dimensional relative position estimation. These results demonstrate that the proposed method can effectively estimate the three-dimensional relative positions of multiple robots, which is the primary objective of this study.

## VI. CONCLUSION

In this study, we propose a ranging system that employs a regular polyhedron to develop a relative position estimation method for mobile robot distributed cooperation systems. Simulations demonstrated that, compared to conventional methods, the proposed approach significantly reduces error. Verification through actual distance measurements confirmed that the proposed method effectively minimizes errors relative to conventional techniques. However, some experimental results from actual ranging showed larger errors than those observed in simulations. This discrepancy is attributed to radio wave interference in the experimental environment. The proposed method is most effective when high-precision ranging is achievable. This technique enables each robot to estimate its position relative to others, which is essential for implementing effective autonomous decentralized control in systems with two or more robots.

## VII. FUTURE WORK

In the future, we will increase the number of faces, compare the accuracies of various polyhedral structures, and implement them in mobile robots as a method for relative position estimation. The proposed approach has the potential to facilitate the deployment of multi-robot systems in environments where GNSS is unavailable, such as underground spaces, indoor settings, and extraterrestrial locations. However, reducing the unit size results in decreased positioning accuracy, highlighting the need for an effective solution to integrate the system into a single device.

## ACKNOWLEDGMENT

We would like to thank Editage (www.editage.com) for English language editing.

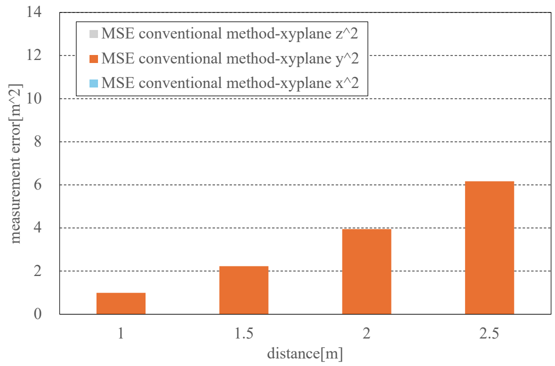


(a) Conventional method (square, $xy$-plane).

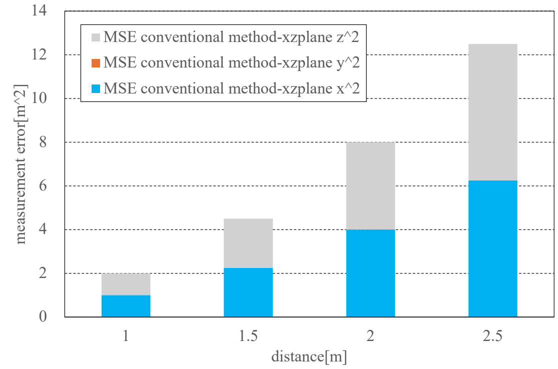


(b) Conventional method (square, $xz$-plane).

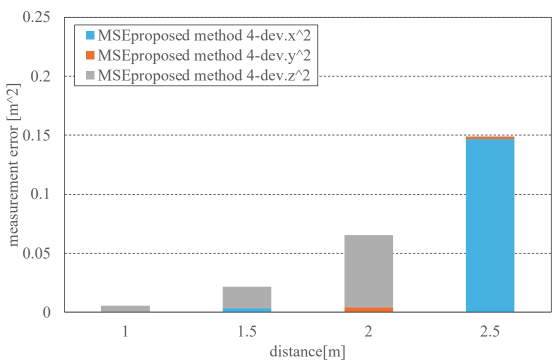


(c) Proposed method with four devices (tetrahedron).

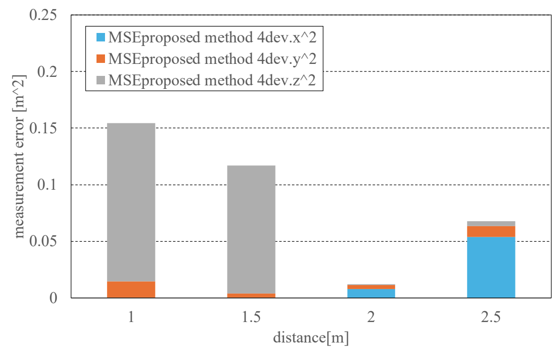


(d) Proposed method with six devices (octahedron).

Fig. 8. Errors caused by squared errors in actual experiments (Side length: 0.5 m).

## REFERENCES


[1] Y. Tan, and Z. Zheng. "Research advance in swarm robotics," Defence Technology vol. 9, pp.18-39, 2013.

[2] Y. Kantaros and M. M. Zavlanos, "Global Planning for Multi-Robot Communication Networks in Complex Environments," IEEE Transactions on Robotics, vol. 32(5), pp. 1045–1061, 2016.

[3] R. K. Ramachandran, J. A. Preiss and G. S. Sukhatme, "Resilience by Reconfiguration: Exploiting Heterogeneity in Robot Teams," 2019 IEEE/RSJ International Conference on Intelligent Robots and Systems (IROS), Macau, China, pp. 6518-6525, 2019.

[4] J. Alonso-Mora, E. Montijano, T. Nägeli, et al., "Distributed multi-robot formation control in dynamic environments," Autonomous Robots, vol. 43, pp. 1079–1100, 2019.

[5] Y. Kiri, M. Sugano, and M. Murata, "Robustness in sensor networks: Difference between self-organized control and centralized control," International Journal on Advances in Networks and Services, vol. 2(1), pp. 45–52, 2009.

[6] L. Zhou, S. Leng, Q. Wang and Q. Liu, "Integrated Sensing and Communication in UAV Swarms for Cooperative Multiple Targets Tracking," IEEE Transactions on Mobile Computing, vol. 22(11), pp. 65260-6542, 2023.

[7] K. Dai, B. Sun, G. Wu, S. Zhao, et al., "LiDAR-Based Sensor Fusion SLAM and Localization for Autonomous Driving Vehicles in Complex Scenarios," Journal of Imaging, vol. 9(2):52, 2023.

[8] E. Héry, X. Philippe, and P Bonnifait. "Consistent decentralized cooperative localization for autonomous vehicles using LiDAR, GNSS, and HD maps," Journal of Field Robotics vol. 38.4, pp. 552–571, 2021.

[9] J. Varela-Aldás, C. Ichina, B. Ruales, and V.H. Andaluz, "Application for the Cooperative Control of Mobile Robots with Energy Optimization," In: Kurosu, M. (eds) Human-Computer Interaction. Interaction Techniques and Novel Applications. HCII 2021. Lecture Notes in Computer Science, vol. 12763. Springer, 2021.

[10] Y. Li, and C. Tan, "A survey of the consensus for multi-agent systems," Systems Science & Control Engineering, vol. 7(1), pp. 468–482, 2019.

[11] J. C. Adams, W. Gregorwich, L. Capots, and D. Liccardo, "Ultra-wideband for navigation and communications," 2001 IEEE Aerospace Conference Proceedings (Cat. No.01TH8542), Big Sky, MT, USA, 2001, vol. 2, pp. 2/785-2/792, 2001.

[12] L. Yao, L. Yao, and Y. Wu, "Analysis and Improvement of Indoor Positioning Accuracy for UWB Sensors," Sensors, Vol. 21(17):5731, 2021.

[13] L. Flueratoru, S. Wehrli, M. Magno, E. S. Lohan and D. Niculescu, "High-Accuracy Ranging and Localization With Ultrawideband Communications for Energy-Constrained Devices," IEEE Internet of Things Journal, vol. 9(10), pp. 7463–7480, 2022.

[14] S. N. A. Ahmed and Y. Zeng, "UWB positioning accuracy and enhancements," IEEE Region 10 Conference, pp. 634–638, 2017.

[15] N. Zhou, M Si, D. Li, C.K. Seow,and J. Mi, "An Indoor UWB 3D Positioning Method for Coplanar Base Stations," Sensors, vol.22(24):9634, 2022.

[16] R. Liu, C. Yuen, T-N. Do, D. Jiao, X. Liu and U-X. Tan, "Cooperative relative positioning of mobile users by fusing IMU inertial and UWB ranging information," IEEE International Conference on Robotics and Automation (ICRA), pp. 5623–5629 , 2017.

[17] T-M. Nguyen, A. Hanif Zaini, C. Wang, K. Guo and L. Xie, "Robust Target-Relative Localization with Ultra-Wideband Ranging and Communication," 2018 IEEE International Conference on Robotics and Automation (ICRA), pp. 2312–2319, 2018.

[18] J. P. Mathew and C. Nowzari, "ReLoki: A Light-Weight Relative Localization System Based on UWB Antenna Arrays," Sensors, vol. 24(16):5407, 2024.

[19] S. Gezici, "A Survey on Wireless Position Estimation," Wireless Pers Commun, vol. 44, pp. 263-–282 ,2008.

[20] C. Cai, et al., "Precise point positioning with quad-constellations: GPS, BeiDou, GLONASS and Galileo," Advances in space research, vol. 56(1), pp. 133–143, 2015.

[21] K. Bregar, "Indoor UWB Positioning and Position Tracking Data Set," Scientific data, Vol. 10(744), 2023.

[22] Qorvo, "QM33120W Product Data Sheet," QM33120W Fully Integrated Impulse Radio Ultra-Wideband (UWB) Wireless Transceiver, Rev. D, 2025.[Online].Available:https://www.qorvo.com/products/p/QM33120W (accessed Jan. 15, 2026).